Polymer conjugated retinoids for controlled transdermal delivery

HHS Public Access

Author manuscript

J Control Release. Author manuscript; available in PMC 2017 October 16.

Published in final edited form as:

J Control Release. 2017 September 28; 262: 1–9. doi:10.1016/j.jconrel.2017.07.003.

Polymer Conjugated Retinoids for Controlled Transdermal Delivery

Steven A. Castleberry[1,2,3,4], **Mohiuddin A. Quadir**[1,2], **Malak Abu Sharkh**[1], **Kevin E. Shopsowitz**[1,2], and **Paula T. Hammond**[1,2,3,*]

[1]Department of Chemical Engineering, Massachusetts Institute of Technology, Cambridge, MA, 02139

[2]Koch Institute of Integrative Cancer Research, Massachusetts Institute of Technology, Cambridge, MA, 02139

[3]Institute for Soldier Nanotechnologies, Massachusetts Institute of Technology, Cambridge, MA, 02139

[4]Harvard-MIT Division of Health Sciences and Technology, Cambridge, MA, 02139

Abstract

All-trans retinoic acid (ATRA), a derivative of vitamin A, is a common component in cosmetics and commercial acne creams as well as being a first-line chemotherapeutic agent. Today, formulations for the topical application of ATRA rely on creams and emulsions to incorporate the highly hydrophobic ATRA drug. These strategies, when applied to the skin, deliver ATRA as a single bolus which is immediately taken up into the skin and contributes to many of the known adverse side-effects of ATRA treatment, including skin irritation and hair loss. Herein we present a new concept in topical delivery of retinoids by covalently bonding the drug through a hydrolytically degradable ester linkage to a common hydrophilic polymer, polyvinyl alcohol (PVA), creating an amphiphilic nanomaterial that is water soluble. This PVA bound ATRA can then act as a pro-drug and accumulate within the skin to allow for the sustained controlled delivery of active ATRA. This approach was demonstrated to release active ATRA out to 10 days *in vitro* while significantly enhancing dermal accumulation of the ATRA in explant pig skin. *In vivo* we demonstrate that the pro-drug formulation reduces application site inflammation compared to free ATRA and retains the drug at the application site at measurable quantities for up to six days.

Keywords

All-trans retinoic acid; poly (vinyl alcohol); polymer conjugate; transdermal drug delivery

*Corresponding author: Paula T. Hammond, Professor, Department of Chemical Engineering, Koch Institute of Integrative Cancer Research, Massachusetts Institute of Technology, Room 76-553, Cambridge, MA 02139, hammond@mit.edu.

Author Contributions: S.C. performed surgeries and experiments, collected and analyzed data, and wrote the manuscript. M.S. and M.Q. assisted in procedures and helped write the manuscript. K.S. assisted in experiments and imaging. P.H. developed and supervised the project. The manuscript was read and approved by all co-authors.

Competing Financial Interests: The authors declare no competing financial interests.

Introduction

All-trans retinoic acid (ATRA), a metabolite of Vitamin A, is a key component in the topical treatment of numerous skin disorders, including: acne, psoriasis, and UV-induced photoaging.[1-8] ATRA therapy acts by reducing abnormal follicular epithelial hyper-keratinization as well as repressing UV-induced cell signaling pathways that lead to upregulated expression of metalloproteinases.[9-14] Use of ATRA however is limited by its serious side-effects such as skin irritation and hair loss as well as its poor chemical stability.[15-20] Previous investigations have looked to control these undesirable characteristics through controlled release formulations such as creams, microparticles, and emulsions.[17, 21-24] These strategies, however, rely on bolus delivery of active ATRA that, in the case of creams and emulsions, can become immediately available. This rapid increase in local concentration causes a number of adverse side-effects;[10, 25]while on the other hand, microparticle approaches require injection across the dermis, increasing the potential for immunologic response and infection. To date, there has been limited research into polymer-conjugated forms of ATRA, with the focus on application in cancer therapies.[26-28]

Poly(vinyl alcohol) (PVA) is an excipient of choice in many pharmacologic formulations and is commonly used in the preparation of biodegradable particles.[29-32] PVA is well tolerated and has demonstrated a very good safety profile *in vivo*.[33-36] Applications for PVA in drug delivery primarily focus on it as a surfactant, providing excellent drug loading while allowing control over particle size and stability.[37-40] Recent reports have highlighted the mucoadhesive nature of PVA coated particles, suggesting that the hydrogen bonding ability of PVA promotes interaction with mucosal proteins.[41-44] This adhesive nature of PVA to mucosal components suggests a broader potential use, one that can take advantage of the hydrogen bonding to increase the residence time of drugs within tissues. Conjugating the hydrophobic ATRA to the very hydrophilic PVA through a hydrolytically degradable ester linkage, creates a new approach to formulate ATRA into a controlled release nanomaterial with potentially enhanced tissue residence.

Controlling ATRA release presents many substantial improvements over the current techniques for ATRA delivery. Currently ATRA is placed as a bolus at the sight of interest, immediately activating retinoic acid receptors and generating a strong pro-inflammatory response that can cause serious pain, irritation, and damage to the dermis. Bolus delivery also requires constant re-application to the sight of interest, often multiple times per day. By delivering ATRA as a controlled-release conjugate, we can avoid these side effects and promote a more healthy response from the tissue with better control over ATRA action.

In this report, we describe the synthesis and evaluation of a PVA-ATRA polymer-drug conjugate (PATRA) for topical controlled delivery of ATRA. When hydrated, PATRA forms a nanoparticle micelle which is soluble in water and provides protection from UV degradation of ATRA. Release of ATRA from the polymer conjugate was sustained for up to ten days *in vitro*. Delivery into skin was evaluated first using explant pig dermis which showed a near four-fold increase in ATRA accumulation within the dermis and a ten-fold reduction in ATRA that fully permeates through the tissue after 12 hours compared to bolus ATRA administration. When tested *in vivo* PATRA was observed to elicit minimal

inflammatory response compared to ATRA therapy, while remaining present for up to nearly five days post-application. These marked improvements in delivery profile, retention, and lowered side effects suggest that PATRA may be a promising new approach to the retinoid treatment.

Methods and Materials

Materials

PVA (M_w ~31 kDa) and ATRA were purchased form Sigma-Aldrich (St. Louis, MO). Phosphate-buffered saline (PBS, 10x), Advanced-MEM, fetal bovine serum, antibiotic-antimycotic solution, and 100 mM L-Glutamine solution were purchased from Life Technologies (Grand Island, NY). AlexaFluor 647 NHS ester was purchased from Life Technologies (Grand Island, NY). NIH-3T3 cells were purchased from ATCC (Manassas, VA).

Fabrication of PATRA

0.138g DMAP (1.12 mmol) and 1.0g PVA (**1**, ~31 kDa) were added to a stirred solution of ATRA (**2**, 0.341 g, 1.14 mmol) in 80 mL of anhydrous DMF, and 20 mL of DMSO. The reaction temperature was cooled to 0°C, and DCC (5.7 mmol) was added to the reaction mixture. A 10% degree of functionalization of all hydroxyl groups from PVA was targeted for conversion. The reaction was allowed to run for 24h (determined by thin-layer chromatographic evaluation), during which the reaction temperature was allowed to reach room temperature. After the stipulated reaction period, DCU precipitate was filtered off, and the filtrate was concentrated *in vacuo* at low pressure, and precipitated in ether.

After centrifugation of the ether suspension at 5000 rpm for 15 minutes, the residue was collected, dissolved in water, and dialyzed against water for 12h to remove any insoluble polar impurities. Lyophilization of the dialyzed product yielded yellowish PATRA conjugate (**3**). ^{1}H NMR (400 MHz, D2O): 3.98-4.02 (m, -CH-OH, PVA), 1.5-2.25 (m, -CH2, PVA); ^{13}C NMR (400 MHz, D_2O): 64.71-67.68 (-CH_2-CH-OH), 164.95 (CH-O-CO-).

In Vitro Analysis of PATRA

Release studies were carried out in a hydroalcoholic solution (50:50 ethanol:water) at two physiologically relevant temperatures, 20°C and 37°C. The impact of ATRA on cell proliferation was assessed by supplementing the media of sub-confluent NIH-3T3 cells with ATRA, PATRA, PVA, and PBS in 24-well plates at concentrations equivalent to 10μM ATRA. ATRA was prepared in a concentrated hydroalcoholic solution of 10 μL. A similar dose of ethanol (5 μL) was added to each treatment group immediately after addition of the testing agents. The cell number calculated from imaging of those wells is used as the reference in the calculation of relative cell density.

Uptake, retention, and penetration of ATRA in pig skin were investigated using a Franz diffusion cell. Skin was harvested from the flanks of adult female Yorkshire pigs 1 hour after sacrifice with subcutaneous fat removed. Skin was sectioned and frozen at -80°C for up to six months prior to use. Skin was prepared for diffusion experiments by thawing in PBS for

one hour after which time all hair on the skin was shaven off. Test samples of skin were cut to 30mm × 30mm square samples and placed into the diffusion cell such that the top of the dermis faced a 3mL testing retention reservoir containing the drug and/or drug components, and the underside faced a 15mL penetration reservoir containing no drug components. All studies were run at room temperature.

Samples were placed into the retention reservoir with a drug concentration of 0.1 mg/mL and followed for up to 12 hours. ATRA concentration was evaluated in both the retention and penetration reservoirs every four hours during this period *via* UV absorbance measurements. ATRA was first solubilized in a concentrated alcohol solution (5mg/mL) prior to being diluted into the retention well. A similar amount of ethanol (60μL) was added to the PATRA retention well to control for ethanol concentration. For both groups, the penetration reservoir was filled with a hydroalcoholic solution so that the ATRA that could penetrate the skin would be soluble for UV absorbance measurement.

In Vivo PATRA Application

All animal studies were approved by the MIT Institutional Animal Care and Use Committee (IACUC). Animals were housed and cared for in the USDA-inspected MIT Animal Facility under federal, state, local, and NIH guidelines for animal care. Six week old Balb/CJ mice (n=18) were purchased from Jackson Laboratories (Bar Harbor, ME). Mice were either used for irritation assessment or for IVIS PATRA retention testing.

Mice used for the assessment of irritation were given each of the two different treatments on 1cm^2 regions of their dorsum, these included PATRA, ATRA, PVA, and PBS. A total of twelve mice were used in this assessment. 50μL of 10 μM ATRA solution was placed on two 1 cm^2 shaved areas on the flanks of a Balb/CJ mouse on either side of midline. PATRA (0.092 mg mL^{-1}) and PVA (0.089 mg mL^{-1}) concentrations were controlled for 10 μM ATRA dosing. These solutions were rubbed into the skin using a cotton-tipped applicator for 30 seconds.

Mice used for PATRA retention testing were given two applications of one material, either PATRA or the unconjugated AF-647 dye, on two 1 cm^2 regions on their dorsum on midline. The material was allowed to adsorb into the skin for 30 minutes and then the mice were cleaned with a wetted towel to remove excess. Mice were imaged daily for up to seven days.

Histology

Tissues were fixed in zinc fixative without formalin for 48 hours. The excised tissues were cut on center and then embedded cut-face down in paraffin. Sections were taken at the wound center and at one further level of 500 μm reaching a total of 1mm sampling length through the application site. At each level an H&E slide was stained. Unstained slides were also taken for potential IHC analysis of the tissue. All sections were 5μm thick. Image analysis was performed using Image J.

Statistics

Statistical analysis was performed between groups using Student's *t*-test and rectified by ANOVA for comparisons between multiple groups. Values are represented as mean ± S.D. A value of $p < 0.05$ was used to indicate statistical significance.

Results

Chemical Synthesis of PVA Conjugated ATRA (PATRA)

By conjugating ATRA (**2**) to a highly water soluble FDA approved polymer through an ester-bond linkage, we can produce a water soluble polymer-drug conjugate for the controlled release of ATRA. The choice of polymer is important in this work as it will determine a great deal of the conjugates final characteristics. We chose to focus our work on poly(vinyl alcohol) (PVA, **1**) as it has been used extensively as a drug excipient and is very well tolerated *in vivo*.[31, 33-35, 45] PVA has been described in numerous previous reports for its highly mucoadhesive nature, due to the number of hydrogen bonds it can form with mucosal polysaccharides. In a similar role, we hope to take advantage of this adhesive nature of PVA to form a topical glue that would hold the conjugate within the administration site for the controlled delivery of ATRA.

Conjugating ATRA to PVA was performed *via* the Steglich esterification process using DCC (N,N′-dicyclohexycarbodiimide) chemistry in a one-pot synthesis as described in the methods section of this chapter (Figure 1). For each equivalent of ATRA (2), 5.0 equivalents of DCC was used with DMAP as a catalyst. Initially, DMF was used as solvent which resulted in a heterogeneous reaction condition for carrying out the esterification. Hence DMSO was added to 20% v/v for enhancing the solubility of the reactant mixture. This purified product, **3** was weighed and the UV absorbance for ATRA was quantified. It was determined that as per the directions described in the methods section PVA functionalization with ATRA reached approximately 3.25 weight percent. We have also found that the solubility of PVA can be increased by using DMAc/5% LiCl as the solvent system.

Conjugating the hydrophobic ATRA to the highly water-soluble PVA through an ester-bond linkage logistically produces an amphiphilic material. In aqueous solution the ATRA moieties along the PVA backbone attempt to isolate themselves away from the solvent, forming a micellar structure. We hypothesized that this micelle structure would allow for significantly increased water solubility of the ATRA so long as it was conjugated to the PVA in PATRA.

This increased water dispersion could be used to investigate new formulations and novel means of delivery into the target tissues. It is important to note here that micelles can be easily disrupted by non-specific interactions with proteins and other biomolecules; we would then expect that while the PATRA may form a micelle in an uncluttered aqueous solution, it would lose this structure *in vivo*. Unlike emulsified formulations of ATRA however, by covalently conjugating ATRA to the much larger PVA, along with PVAs mucoadhesive nature, we should be able to retain the conjugate within the application site to achieve controlled release of ATRA (Figure 2).

Characterization of PATRA *In Vitro*

We hypothesized that the covalent conjugation of ATRA to PVA would result in the creation of a water soluble drug-polymer conjugate that would naturally form a micellar structure in aqueous solution. To investigate these hypotheses we performed a series of *in vitro* analyses on the PATRA molecule. We began by gross examination of the purified product, which was a light yellow in color, a lighter shade than the pure ATRA product. PATRA was solubilized in water for ten minutes and then analyzed for the formation of nanoparticles as well as for its general appearance (Figure 3a&c). Nanoparticle structures were observed by dynamic light scattering (DLS) at concentrations starting at 50mg/mL and lower. These particles were in the range of 120 to 150 nm in diameter. The appearance of these particles containing solutions was a light yellow, and was observed to vary in intensity with the relative dilution of the PATRA.

We believed that the logical structure of the PATRA material in aqueous solution was a colloidal structure, however we were unsure what type of a micelle would be formed. To investigate this important characteristic we performed transmission electron microscopy of the PATRA using uranyl acetate negative staining to mark the hydrophobic ATRA-rich regions of the structure, which appear dark in the TEM micrographs (Figure 3b). What we observe is a nano-fibrillar structure, where ATRA is occluded in the center of a thin high aspect ratio cylindrical micelle. These fiber structures are only a few nanometers in diameter, while being tens of nanometers in length. The nanofibers agglomerate into particles that are similar in size to the 120 to 150 nm structures we observed by DLS measurement.

As the PATRA polymer appeared to better solubilize the ATRA molecule in water, we were interested in determining the extent of this increased solubility. We thus investigated the solubility of free ATRA and PATRA in three different solutions: (1) hydroalcoholic (50:50), (2) deionized water, and (3) PBS 1x (pH7.4). Solubility was evaluated by bringing 2mg/ml of ATRA either free or conjugated to PVA into equilibrium at room temperature for 1 hour, followed by centrifugation of the solution at 1,500 rpm for five minutes to remove any undissolved precipitate (Figure 3d). The supernatant from this process was then used for the testing of ATRA concentration *via* UV absorbance as previously described.[25]

ATRA was observed to be insoluble in deionized water and PBS solutions. In contrast, PATRA quickly dissolved into water and PBS, achieving visibly clear yellow solutions within minutes. PATRA was able to support concentration up to 0.33 ± 0.08 mg/mL ATRA stably in deionized water and 0.35 ± 0.04 mg/mL into PBS. These quantities were notably less than what we had previously observed from our solubility studies, suggesting that those findings may have included material that was able to be removed by centrifugation. These materials could include partially solubilized polymers as well as large micro-aggregates of the micelles.

We also investigated the relative stability of the micelle structure by evaluating it in simulated body fluids. We did this by the addition of 5% fetal bovine serum (FBS) into deionized water or PBS solutions of PATRA. What we observed was a complete loss of the particle signal within the solution, generating a wide heterogeneous signal that was uninterpretable by DLS. This suggests that the presence of the proteins within the FBS could

drive the disassembly of the micelle structure. This is important as one would assume that upon entry into the skin the presence of proteins and other macromolecules would operate similarly and drive the disassembly of the micelle structure *in vivo*. A similar loss of particle structure was observed with the addition of ethanol to PATRA solubilized in water. By DLS the particle distribution was very broad from multiple microns to tens of nanometers in scale for PATRA in the hydroalcoholic solution.

Controlled Release of ATRA

Release of ATRA from the PATRA polymer was evaluated by dialysis. The PVA polymer is ~31 kDa and the ATRA molecule is only 300 Da; therefore, carrying out the release of ATRA within a dialysis bag with a 10 kDa cutoff enabled retention of the PATRA and PVA while isolating the ATRA. Release was carried out in hydroalcohol solution as this solvent mixture created a similar loss of particle structure as what we would hypothesize to happen *in vivo* and solubilizes the released ATRA so that we can continuously track its release *in situ*.

Release studies were carried out at two physiologically relevant temperatures as it is known that ester hydrolysis is affected by temperature (Figure 4a). We chose to consider 20°C and 37°C as these would approximately represent room temperature and body temperature for the application of the PATRA formulation. Daily measurements of the released ATRA demonstrated a continuous liberation of the ATRA into solution over approximately eight days.

We investigated the in vitro stability of the PATRA micelles in water, as storage of the formed micelles in water would likely lead to release of ATRA. We evaluated this property by simply solubilizing PATRA within deionized water and evaluating the average particle diameter over time. It was observed that the average particle diameter increased with storage significantly over a 100 hour study period (Figure 4b). During this time it was also observed that the size distribution of particles widened. One possible explanation for this behavior is that as ATRA is released, the highly hydrophobic molecule becomes sequestered within the hydrophobic interior regions of the PATRA micelles over time. This explanation addresses the observed widening of particle size distribution upon storage of PATRA for long time periods in water; released ATRA causes inter/intramolecular aggregation within PATRA fibers, thus widening the distribution. The sequestration of released molecules in the existing micelles could act as a secondary mechanism of controlled release, and may also explain why significant differences in free molecule release were not observed between room and body temperature for these systems.

In Vitro Activity of PATRA

The *in vitro* activity of ATRA was measured by evaluating its effect as an anti-proliferative, as has been previously reported.[18, 20, 46] This was done by supplementing the media of sub-confluent NIH-3T3 cells with ATRA, PATRA, PVA, and control solution in 24-well plates at concentrations equivalent to 10 μM ATRA. ATRA is not soluble in water, and as such must be solubilized in a concentrated hydroalcoholic solution which is then added to cell culture. Ethanol, even in a very low concentration, can be detrimental to cell survival

and proliferation. For this reason a similar dose of ethanol was added to each treatment group immediately after addition of the testing agents. The control solution is deionized water with a small control volume of ethanol, and the cell number calculated from imaging of those wells is used as the reference in the calculation of relative cell density.

Cell proliferation was measured by daily brightfield phase contrast imaging for up to four days as well as with metabolic activity assay after the four days in culture. PATRA was observed to achieve a similar decrease in proliferation as ATRA, while PVA treatment caused negligible changes in proliferation (Figure 5). The level of anti-proliferative activity observed in PATRA treated cultures suggests that the activity of ATRA *in vitro* is not inhibited by its conjugation to PVA. It is also possible that PATRA may operate in a different fashion than free ATRA. A third option is that in the presence of cells, hydrolysis of the PATRA ester bond may be accelerated, liberating bound ATRA.

Ex Vivo Delivery of PATRA

To achieve an effective treatment for dermatological applications, it is important to achieve appropriate pharmacokinetics and accumulation of ATRA in the epidermis layer of the skin, where it creates a ‘depot-like’ environment for controlled delivery. Uptake, retention, and penetration of ATRA in pig skin were investigated using a Franz diffusion cell using previously described. In brief, skin was harvested from the flanks of adult female Yorkshire pigs 1 hour after sacrifice with subcutaneous fat removed. Skin was sectioned and frozen at -80°C for up to six months prior to use. Skin was prepared for diffusion experiments by thawing in PBS for one hour after which time all hair on the skin was shaven off. Test samples of skin were cut to 30mm × 30mm square samples that were placed into the diffusion cell such that the top of the dermis was facing a 3mL testing retention reservoir and the underside faced a 15mL penetration reservoir. All studies were run at room temperature.

Samples to be tested were placed into the retention reservoir at a concentration of 0.1 mg/mL and followed for up to 12 hours. ATRA concentration was evaluated in both the retention and penetration reservoirs every four hours during this period *via* UV absorbance measurements. Similar to what had been done for *in vitro* studies; ATRA was first solubilized in a concentrated alcohol solution prior to being diluted into the retention well. A similar amount of ethanol was added to the PATRA retention well to control for this. For both groups the penetration reservoir was filled with a hydroalcoholic solution so that the ATRA that penetrated the skin would be soluble for UV absorbance measurements.

The structure of the pig skin is shown in Figure 6a. The uppermost layer is the stratum corneum, followed by the epidermis and then the dermis. Each of these layers presents a different environment for ATRA and PATRA accumulation. We labeled the PATRA with a fluorescent dye to determine where the PATRA localizes within the skin. What we observed was an increasing concentration of PATRA within the epidermis over the testing period (Figure 6b). After four hours the tissue looks largely unremarkable, with some fluorescent signal appearing in the stratum corneum. After 12 hours, an intense clear signal throughout the epidermis is observed, indicating a significant enrichment of this portion of the skin for the labeled PATRA.

Following the ATRA concentration within the receiving reservoir on the underside of the pig skin (amount fully penetrated), we observed a much higher level of ATRA accumulation at every time point tested for free ATRA than PATRA (Figure 6c). Logically, this makes sense as the diffusion of the much larger PATRA molecule would be much slower than the smaller ATRA molecule. In addition to this significant property change, the nature of PVA to form hydrogen bonds within the tissue may lower net diffusion and thus also be contributing to this impaired penetration.

Quantification of the ATRA concentration within the retention and penetration reservoirs allows us to perform a mass balance analysis for the ATRA in the testing system. This analysis showed that there was a significantly higher accumulation of the PATRA within the pig skin than was observed for free ATRA (Figure 6d). After 12 hours of exposure, approximately 8.2 ± 1.1% of the ATRA placed in the retention reservoir had accumulated within the treated skin, with the amount increasing over the test period, compared to only 1.9 ± 0.9% of free ATRA. This finding is in agreement with our previous findings from labeled PATRA, in which we had observed accumulation within the epidermis over this period of time.

In Vivo PATRA Causes Less Irritation

One of the most reported side effects of topical ATRA therapy is irritation within the application region. This is due in large part to the bolus administration of ATRA, which can often reach super-therapeutic levels easily, especially when treatments require multiple daily administrations of the ATRA formulation. To investigate the relative irritative nature of PATRA in comparison to ATRA we tested each on the flanks of mice. Irritation was evaluated by digital imaging of the application site of ATRA, PATRA, or control solutions for up to five days post-application as well as by histological evaluation of inflammation after 5 days. In brief, 50μL of 10 μM ATRA solution was placed on a 1 cm^2 shaved area on the flank of a Balb/CJ mouse. PATRA (0.092 mg mL^{-1}) and PVA (0.089 mg mL^{-1}) concentrations were controlled for 10 μM ATRA dosing. This solution is rubbed into the skin using a cotton-tipped applicator for 30 seconds. Each mouse received one of the four different material solutions applied in two locations. Inflammation and dermal changes subsequent to ATRA application were evaluated by both by digital imaging and by H&E histology.

Grossly, the ATRA treated skin begins to appear inflamed after three days, developing a thick and rough appearance (Figure 7a). The stratum corneum thickens and has a crust like presentation, with flakes missing, giving a rash like appearance to the site of application. The PATRA and PVA treated skin sections have no such change in appearance. After five days of treatment the ATRA treated skin looks less irritated with fewer red spots observed on the skin surface, however it still has a rash-like quality with a thick and calloused appearance. Neither the PATRA nor the PVA treated skin has any such changes. These application sites appear the same as they did prior to application and are very similar to control treated skin.

Histologically, the differences between the treatment groups can be easily appreciated (Figure 7b-d). Significantly increased stratum corneum (SC) and epidermal thickness was

observed in ATRA treated mice, while not seen in PATRA or control group subjects, indicating increased inflammation within these tissues. *In vivo* evaluation of PATRA-induced irritation showed a significant reduction in both the irritation and inflammation as seen in similar ATRA applications. We believe this is due to the controlled manner in which the ATRA is released from PATRA, reducing the likelihood of over-stimulating the dermis with ATRA upon administration.

Improved In Vivo Retention of PATRA

The application and retention of the PATRA material was followed using a dye-conjugated form of PATRA. This material was prepared similarly to the base PATRA with the inclusion of an alexafluor-647 dye that was bound to PVA through an ester-linkage, similar to the ATRA molecule. Whole-animal *in vivo* imaging for the tracking of the labeled conjugate was performed on a daily basis for seven days. As a control for the dye-conjugated PATRA, we also similarly deposited the free dye on the dorsum of mice to track the loss of the free dye signal.

PATRA and the small molecule dye were both applied to the backs of mice in two locations on the midline on day 0. The materials were allowed to absorb into the skin for 30 minutes and then the backs of the mice were washed twice using a wet cloth. Average radiant efficiency was quantified within the area of application (Figure 8a-b). It was observed that the labeled PATRA showed a 3-fold longer half-life within the skin versus the unconjugated small molecule fluorescent dye. The signal from the dye-conjugated PATRA could be seen to persist for out to five days with the average time to 95% clearance lasting almost 6 days (Figure 8c).

Discussion

Topical application of all-trans retinoic acid is commonly used to treat severe acne and psoriasis as well as being used in many cosmetic applications for its anti-photoaging effects.[6, 14, 47, 48] Administration of ATRA however, presents many difficulties due to its hydrophobic nature and poor stability. A number of different approaches to delivering ATRA to the dermis have been previously investigated.[25, 27, 49, 50] These approaches have focused on formulating ATRA with emulsifiers and lipids to improve solubility or entrapping it within polymer-based particles to provide sustained release. Achieving both high solubility and controlled release of ATRA from a single platform is thus a challenging task.

Here we have presented a new approach to address these issues by directly conjugating ATRA to PVA through a hydrolytically degradable ester-bond linkage. This conjugate formulation helps to solubilize ATRA in water while improving retention of the small molecule at the application site. The approach developed within this work is a simple and robust method using DCC chemistry to form a polymer-drug conjugate which provides a great deal of optimization flexibility in formulation design.

In vitro evaluation of ATRA release demonstrated sustained release for over ten days with little to no reduction in activity over that time. When hydrated, PATRA forms high aspect

ratio nanofibers that agglomerate into larger submicron scale nanoparticles. Uptake and retention of the conjugated ATRA was significantly increased over the free ATRA for experiments using explant pig skin, and was observed to accumulate within the epidermal layer of the skin, increasing throughout the study period. Applying the PATRA conjugate *in vivo* we observed a significant reduction in gross inflammation compared to free ATRA as well as a reduction in histological signs for inflammation. Further, we investigated the retention of PATRA on the skin, and demonstrated that this conjugated formulation remains at measurable levels at the site of application for up to three days.

This data taken together presents a substantial argument for the capability of this described method to effectively control the delivery of ATRA into the dermis for topical applications. This style of approach may also be more broadly applicable for controlling ATRA delivery in combination with a number of existing formulations including emulsion and cream technologies. We also believe that the self-assembled PATRA nano-fibers may present some beneficial properties for incorporation of ATRA in nanoparticle formulations for cancer therapy.

Acknowledgments

The authors would like to thank Carl Schoellhammer for his help in setting up *ex vivo* pig skin transport experiments. This research was supported in part by funding and core facilities provided by the U.S. Army Research Office under contract W911NF-07-D-0004 at the MIT Institute of Soldier Nanotechnology. This work was also supported by use of core facilities at the Koch Institute for Integrative Cancer Research (supported by the NCI under grant 2P30CA014051-39). We thank the Koch Institute Swanson Biotechnology Center for technical support, specifically the microscopy, flow cytometry, and histology cores. M.Q. acknowledges the support of Misrock Foundation Postdoctoral Fellowship for this work. The authors wish to dedicate this paper to the memory of Officer Sean Collier, for his caring service to the MIT community and for his sacrifice.

References

1. Gollnick H, Schramm M. Topical drug treatment in acne. Dermatology. 1998; 196:119–125. [PubMed: 9557245]
2. Orfanos CE, Ehlert R, Gollnick H. The Retinoids - a Review of Their Clinical-Pharmacology and Therapeutic Use. Drugs. 1987; 34:459–503. [PubMed: 3315625]
3. Mills OH, Kligman AM. Treatment of Acne-Vulgaris with Topically Applied Erythromycin and Tretinoin. Acta Derm-Venereol. 1978; 58:555–557. [PubMed: 83088]
4. Olsen EA, Katz HI, Levine N, Shupack J, Billys MM, Prawer S, Gold J, Stiller M, Lufrano L, Thorne EG. Tretinoin Emollient Cream - a New Therapy for Photodamaged Skin. J Am Acad Dermatol. 1992; 26:215–224. [PubMed: 1552056]
5. Lehman PA, Slattery JT, Franz TJ. Percutaneous-Absorption of Retinoids - Influence of Vehicle, Light Exposure, and Dose. J Invest Dermatol. 1988; 91:56–61. [PubMed: 3385216]
6. Fisher GJ, Datta SC, Talwar HS, Wang ZQ, Varani J, Kang S, Voorhees JJ. Molecular basis of sun-induced premature skin ageing and retinoid antagonism. Nature. 1996; 379:335–339. [PubMed: 8552187]
7. Sporn MB, Roberts AB, Roche NS, Kagechika H, Shudo K. Mechanism of action of retinoids. J Am Acad Dermatol. 1986; 15:756–764. [PubMed: 3021829]
8. Panabierecastaings MH. Retinoic Acid in the Treatment of Keloids. J Dermatol Surg Onc. 1988; 14:1275–1276.
9. Montenegro L, Panico AM, Ventimiglia A, Bonina FP. In vitro retinoic acid release and skin permeation from different liposome formulations. Int J Pharm. 1996; 133:89–96.

10. Yamaguchi Y, Nagasawa T, Nakamura N, Takenaga M, Mizoguchi M, Kawai S, Mizushima Y, Igarashi R. Successful treatment of photo-damaged skin of nano-scale atRA particles using a novel transderinal delivery. J Control Release. 2005; 104:29–40. [PubMed: 15866332]
11. Shin SC, Kim HJ, Oh IJ, Cho CW, Yang KH. Development of tretinoin gels for enhanced transdermal delivery. Eur J Pharm Biopharm. 2005; 60:67–71. [PubMed: 15848058]
12. Pedace FJ, Stoughto R. Topical Retinoic Acid in Acne Vulgaris. Brit J Dermatol. 1971; 84:465. &. [PubMed: 4253593]
13. Yavuzer RF, Sen T, Tarimci N, Birol A. Improved efficacy and tolerability of retinoic acid in acne vulgaris. J Am Acad Dermatol. 2004; 50:P20–P20.
14. Harris DWS, Buckley CC, Ostlere LS, Rustin MHA. Topical Retinoic Acid in the Treatment of Fine Acne Scarring. Brit J Dermatol. 1991; 125:81–82. [PubMed: 1831384]
15. Das S, Ng WK, Kanaujia P, Kim S, Tan RB. Formulation design, preparation and physicochemical characterizations of solid lipid nanoparticles containing a hydrophobic drug: effects of process variables. Colloids Surf B Biointerfaces. 2011; 88:483–489. [PubMed: 21831615]
16. Liu J, Hu W, Chen H, Ni Q, Xu H, Yang X. Isotretinoin-loaded solid lipid nanoparticles with skin targeting for topical delivery. Int J Pharm. 2007; 328:191–195. [PubMed: 16978810]
17. Jenning V, Gohla SH. Encapsulation of retinoids in solid lipid nanoparticles (SLN). J Microencapsul. 2001; 18:149–158. [PubMed: 11253932]
18. Puppi D, Piras AM, Detta N, Dinucci D, Chiellini F. Poly(lactic-co-glycolic acid) electrospun fibrous meshes for the controlled release of retinoic acid. Acta Biomater. 2010; 6:1258–1268. [PubMed: 19683605]
19. Brinckerhoff CE, Sporn MB. Retinoids and rexinoids for the 21st century: a brave new world for arthritis. J Rheumatol. 2003; 30:211–213. [PubMed: 12563669]
20. Giordano GG, Refojo MF, Arroyo MH. Sustained delivery of retinoic acid from microspheres of biodegradable polymer in PVR. Invest Ophthalmol Vis Sci. 1993; 34:2743–2751. [PubMed: 8344796]
21. Tadros T, Izquierdo P, Esquena J, Solans C. Formation and stability of nano-emulsions. Adv Colloid Interface Sci. 2004; 108-109:303–318. [PubMed: 15072948]
22. Lira AAM, Rossetti FC, Nanclares DMA, Neto AF, Bentley MVLB, Marchetti JM. Preparation and characterization of chitosan-treated alginate microparticles incorporating all-trans retinoic acid. J Microencapsul. 2009; 26:243–250. [PubMed: 18923964]
23. Castro GA, Oliveira CA, Mahecha GAB, Ferreira LAM. Comedolytic effect and reduced skin irritation of a new formulation of all-trans retinoic acid-loaded solid lipid nanoparticles for topical treatment of acne. Arch Dermatol Res. 2011; 303:513–520. [PubMed: 21298279]
24. Belknap BS. Treatment of Acne with 5-Percent Benzoyl Peroxide Gel or 0.05-Percent Retinoic Acid Cream. Cutis. 1979; 23:856–859. [PubMed: 157264]
25. Shah KA, Date AA, Joshi MD, Patravale VB. Solid lipid nanoparticles (SLN) of tretinoin: potential in topical delivery. Int J Pharm. 2007; 345:163–171. [PubMed: 17644288]
26. Hou L, Yao J, Zhou J, Zhang Q. Pharmacokinetics of a paclitaxel-loaded low molecular weight heparin-all-trans-retinoid acid conjugate ternary nanoparticulate drug delivery system. Biomaterials. 2012; 33:5431–5440. [PubMed: 22521488]
27. Tran TH, Bae BC, Lee YK, Na K, Huh KM. Heparin-folate-retinoic acid bioconjugates for targeted delivery of hydrophobic photosensitizers. Carbohydr Polym. 2013; 92:1615–1624. [PubMed: 23399198]
28. Varshosaz J, Sadeghi-aliabadi H, Ghasemi S, Behdadfar B. Use of magnetic folate-dextran-retinoic acid micelles for dual targeting of doxorubicin in breast cancer. Biomed Res Int. 2013; 2013:680712. [PubMed: 24381941]
29. Chiellini E, Corti A, D'Antone S, Solaro R. Biodegradation of poly (vinyl alcohol) based materials. Prog Polym Sci. 2003; 28:963–1014.
30. Kaneo Y, Hashihama S, Kakinoki A, Tanaka T, Nakano T, Ikeda Y. Pharmacokinetics and biodisposition of poly(vinyl alcohol) in rats and mice. Drug Metab Pharmacokinet. 2005; 20:435–442. [PubMed: 16415529]

31. Paradossi G, Cavalieri F, Chiessi E, Spagnoli C, Cowman MK. Poly(vinyl alcohol) as versatile biomaterial for potential biomedical applications. J Mater Sci-Mater M. 2003; 14:687–691. [PubMed: 15348409]
32. Peppas NA, Scott JE. Controlled Release from Poly(Vinyl Alcohol) Gels Prepared by Freezing-Thawing Processes. J Control Release. 1992; 18:95–100.
33. Nair B. CIRE panel. Final report on the safety assessment of polyvinyl alcohol. Int J Toxicol. 1998; 17:67–92.
34. Jiang Y, Schadlich A, Amado E, Weis C, Odermatt E, Mader K, Kressler J. In-vivo studies on intraperitoneally administrated poly(vinyl alcohol). J Biomed Mater Res B Appl Biomater. 2010; 93:275–284. [PubMed: 20119945]
35. Kobayashi M, Chang YS, Oka M. A two year in vivo study of polyvinyl alcohol-hydrogel (PVA-H) artificial meniscus. Biomaterials. 2005; 26:3243–3248. [PubMed: 15603819]
36. Weis C, Odermatt EK, Kressler J, Funke Z, Wehner T, Freytag D. Poly(vinyl alcohol) membranes for adhesion prevention. J Biomed Mater Res B. 2004; 70B:191–202.
37. Rawat S, Gupta P, Kumar A, Garg P, Suri CR, Sahoo DK. Molecular Mechanism of Poly(vinyl alcohol) Mediated Prevention of Aggregation and Stabilization of Insulin in Nanoparticles. Mol Pharm. 2015
38. Orienti I, Bigucci F, Gentilomi G, Zecchi V. Self-assembling poly(vinyl alcohol) derivatives, interactions with drugs and control of release. J Pharm Sci. 2001; 90:1435–1444. [PubMed: 11745795]
39. Orienti I, Zuccari G, Fini A, Rabasco AM, Montaldo P, Raffaghello L, Carosio R. Modified doxorubicin for improved encapsulation in PVA polymeric micelles. Drug Deliv. 2005; 12:15–20. [PubMed: 15801716]
40. Yamaoka T, Tabata Y, Ikada Y. Comparison of body distribution of poly(vinyl alcohol) with other water-soluble polymers after intravenous administration. J Pharm Pharmacol. 1995; 47:479–486. [PubMed: 7674130]
41. Yang M, Lai SK, Yu T, Wang YY, Happe C, Zhong WX, Zhang M, Anonuevo A, Fridley C, Hung A, Fu J, Hanes J. Nanoparticle penetration of human cervicovaginal mucus: The effect of polyvinyl alcohol. J Control Release. 2014; 192:202–208. [PubMed: 25090196]
42. Ensign LM, Cone R, Hanes J. Oral drug delivery with polymeric nanoparticles: The gastrointestinal mucus barriers. Adv Drug Deliver Rev. 2012; 64:557–570.
43. Mert O, Lai SK, Ensign L, Yang M, Wang YY, Wood J, Hanes J. A poly(ethylene glycol)-based surfactant for formulation of drug-loaded mucus penetrating particles. J Control Release. 2012; 157:455–460. [PubMed: 21911015]
44. Suk J, Kim AJ, Schneider CS, Cebotaru L, Boyle MP, Guggino W, Hanes J. Mucus-Penetrating Nanoparticle for Inhaled Gene Therapy for Cystic Fibrosis. Pediatr Pulm. 2013; 48:256–256.
45. DeMerlis CC, Schoneker DR. Review of the oral toxicity of polyvinyl alcohol (PVA). Food Chem Toxicol. 2003; 41:319–326. [PubMed: 12504164]
46. Jeong YI, Song JG, Kang SS, Ryu HH, Lee YH, Choi C, Shin BA, Kim KK, Ahn KY, Jung S. Preparation of poly(DL-lactide-co-glycolide) microspheres encapsulating all-trans retinoic acid. Int J Pharm. 2003; 259:79–91. [PubMed: 12787638]
47. Reynolds CP, Matthay KK, Villablanca JG, Maurer BJ. Retinoid therapy of high-risk neuroblastoma. Cancer Lett. 2003; 197:185–192. [PubMed: 12880980]
48. Wilkinson RD. Retinoic Acid in Acne Therapy - Reply. Can Med Assoc J. 1976; 114:412–412.
49. Choi Y, Kim SY, Kim SH, Lee KS, Kim C, Byun Y. Long-term delivery of all-trans-retinoic acid using biodegradable PLLA/PEG-PLLA blended microspheres. Int J Pharm. 2001; 215:67–81. [PubMed: 11250093]
50. Manconi M, Sinico C, Valenti D, Loy G, Fadda AM. Niosomes as carriers for tretinoin. I. Preparation and properties. Int J Pharm. 2002; 234:237–248. [PubMed: 11839454]

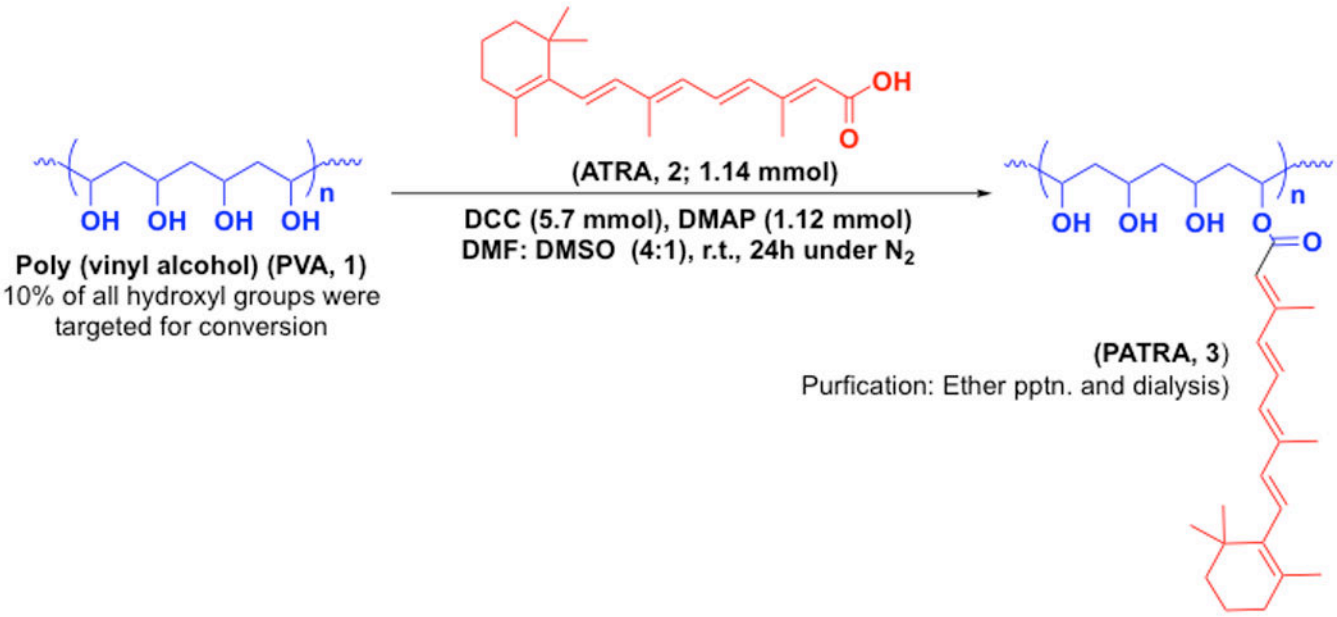

Figure 1. Chemical synthesis of PATRA (3)

Conjugation of ATRA (**2**) to PVA (**1**) was performed using DCC chemistry in DMF:DMSO mixture for 24h at room temperature under nitrogen.

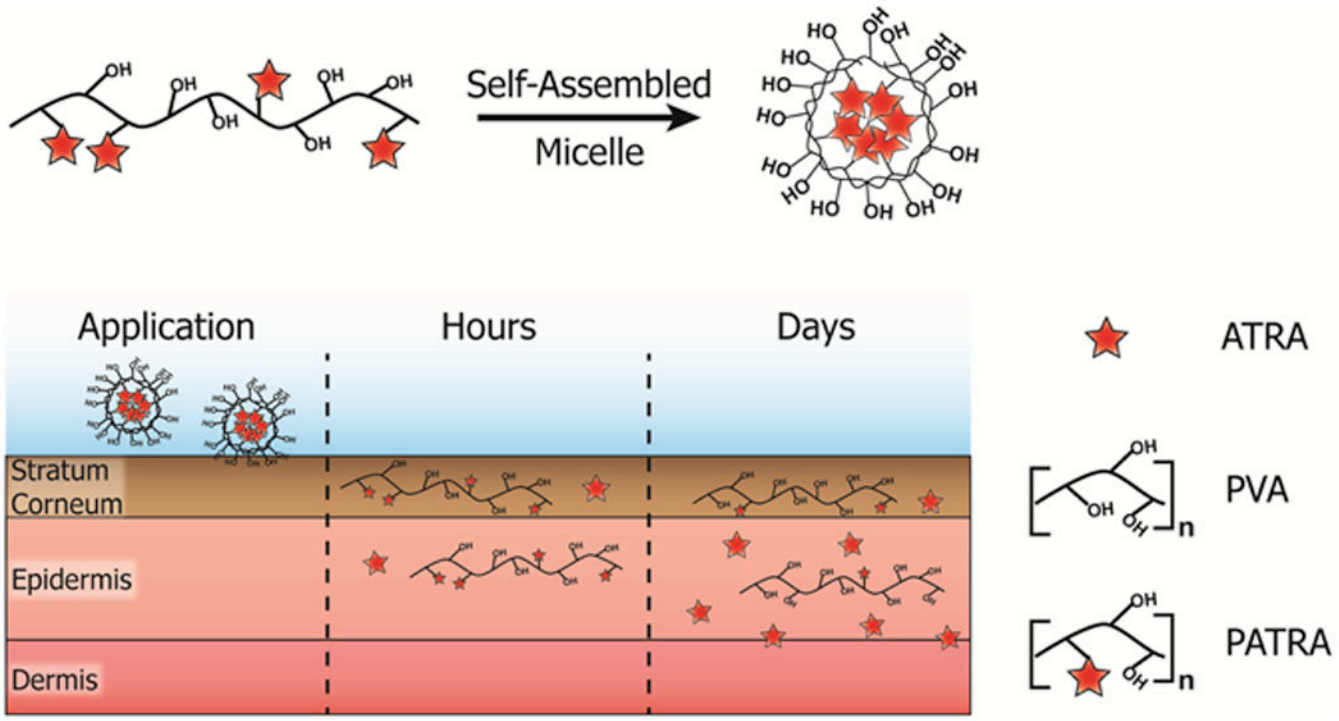

Figure 2. Cartoon schematic of the adsorption of micellar PATRA into the dermis
Release of ATRA from the PATRA conjugate occurs in the hydrated dermis.

A

Polymer (mg/mL)	ATRA (mg/mL)	Particle Diameter (nm)	Appearance
100.0	2.45	N/A	Opaque Yellow
50.0	1.23	126.6 ± 4.1	Clear Yellow
25.0	0.61	131.1 ± 3.2	Clear Yellow
5.0	0.12	138.2 ± 5.1	Clear Yellow
1.0	0.02	148.1 ± 7.2	Clear Light Yellow

B

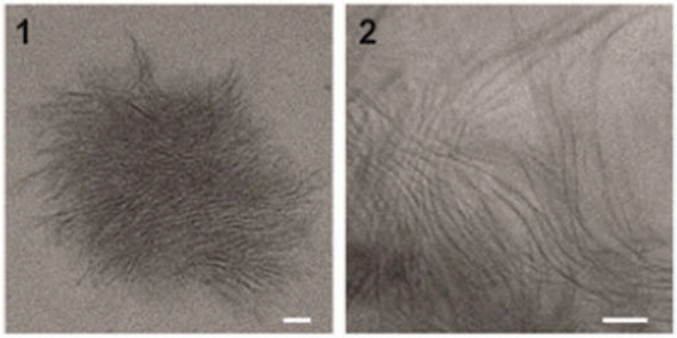

C

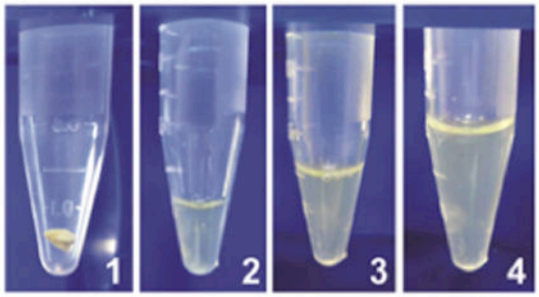

D

Solvent	ATRA Solubility (mg/mL)	PATRA Solubility (mg/mL)
Hydroalcoholic	0.67 ± 0.05	0.58 ± 0.07
Water	< 0.01	0.33 ± 0.08
PBS	< 0.01	0.35 ± 0.04

Figure 3. Nanofiber PATRA solubility and characterization

(a) Characterization of particle size and solution appearance for different concentrations of PATRA in water. (b) TEM images of nano-fiber PATRA formed in water. In water PATRA forms thin (3-5 nm) fibers (2) that agglomerate into nanoparticles (1). (c) Digital images of solubilization of PATRA dry powder (1) at 50mg/mL (2), 25mg/mL (3), and 5mg/mL (4) concentrations. (d) Solubility of ATRA and PATRA in different solutions. Data shown is mean ± S.D., n=3.

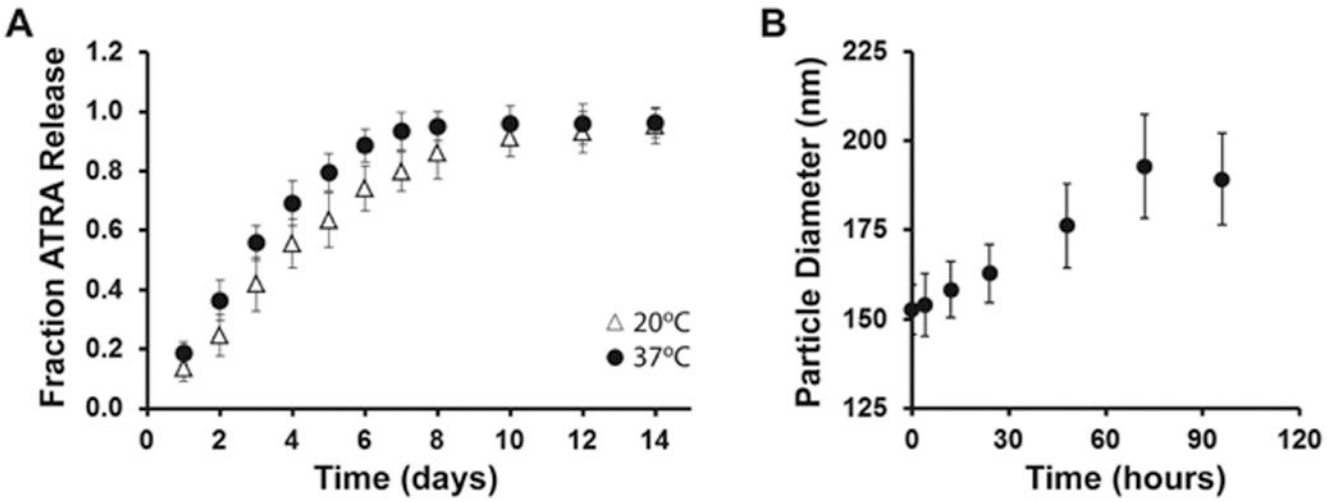

Figure 4. Controlled release of ATRA from PATRA and changes in particle size

(a) ATRA release followed daily at 20°C and at 37°C in hydroalcoholic solution out to two weeks. (b) Average particle size after degrading in water for specified periods of time. Data shown is mean ± S.D., n=3.

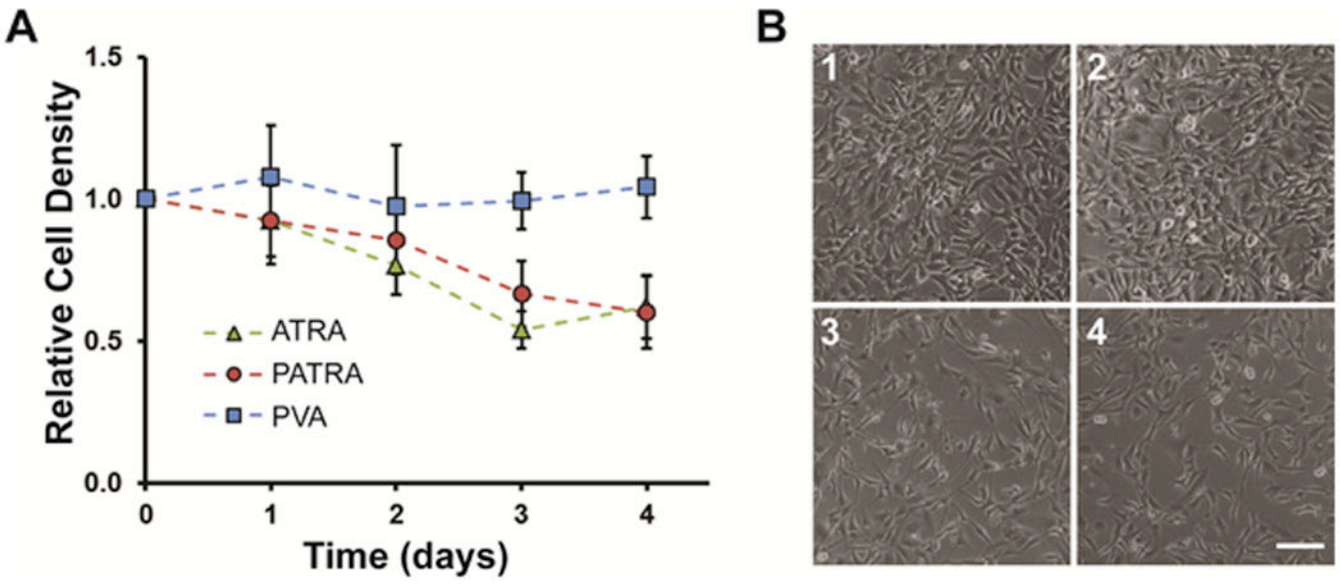

Figure 5. Comparison of impact of ATRA and PATRA on cell viability

(a) Relative cell density of cell cultures treated with ATRA, PATRA, or PVA. ATRA in-well concentration was set at 10μM and PATRA concentration was set at an equivalent ATRA concentration. The concentration of PVA was determined by the PVA concentration in PATRA treated wells. (b) Brightfield imaging after four days in culture of NIH-3T3 cells that are either untreated (1) or treated with (2) PVA, (3) PATRA, (4) ATRA. Scale bar = 50 μm. Data shown is mean ± S.D., n=5.

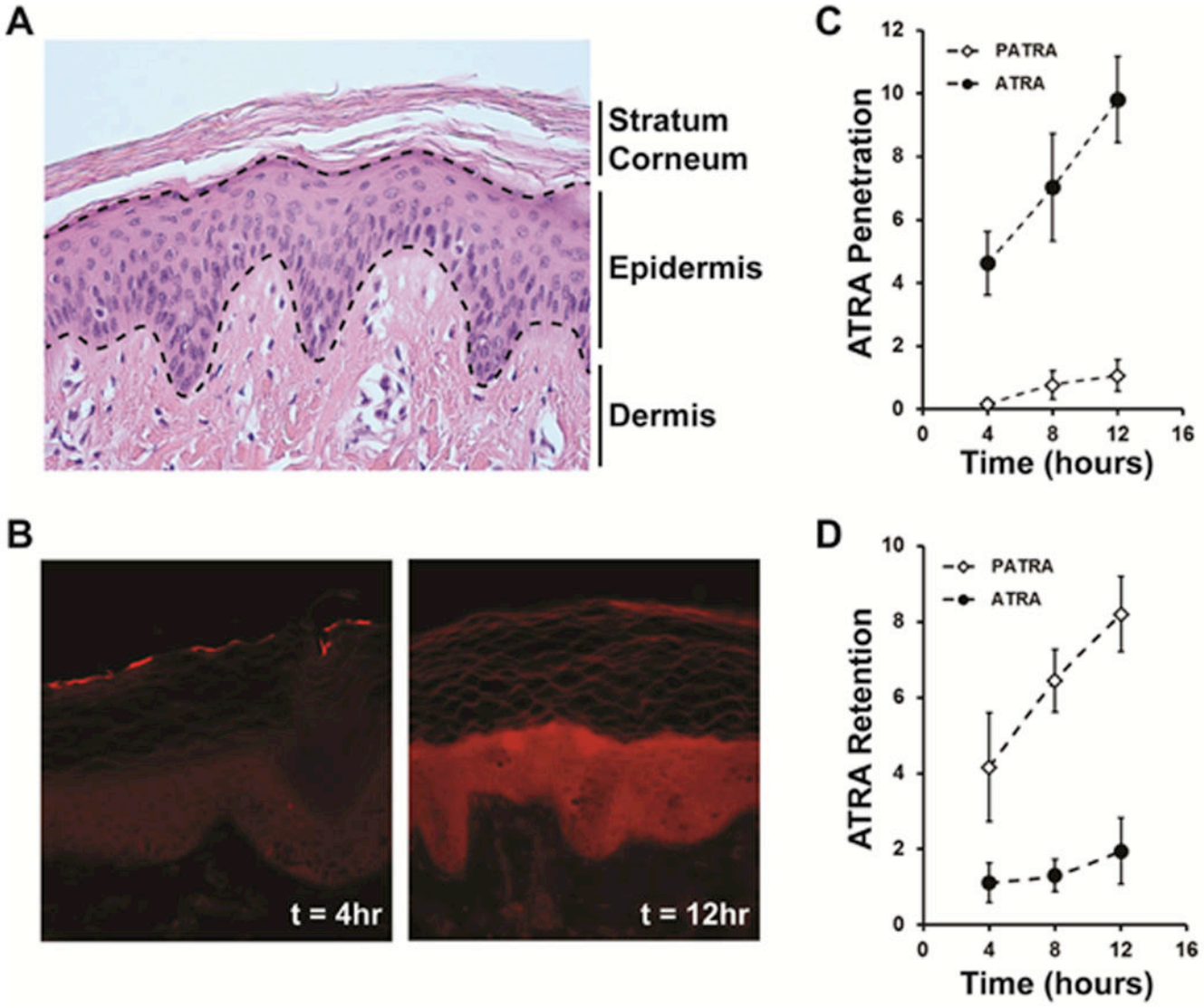

Figure 6. Uptake and transport of ATRA in explant pig skin

(a) Histological appearance of pig dermis. (b) Uptake of fluorescently labeled PATRA after 4 and 12 hours of exposure. Uptake is seen to significantly increase over this time and accumulate within the epidermis. (c) Fraction penetration of ATRA through pig dermis followed over 12 hours. (d) Quantification of fraction of ATRA accumulated within the pig dermis over 12 hours of exposure. Data shown is mean ± S.D., n=4.

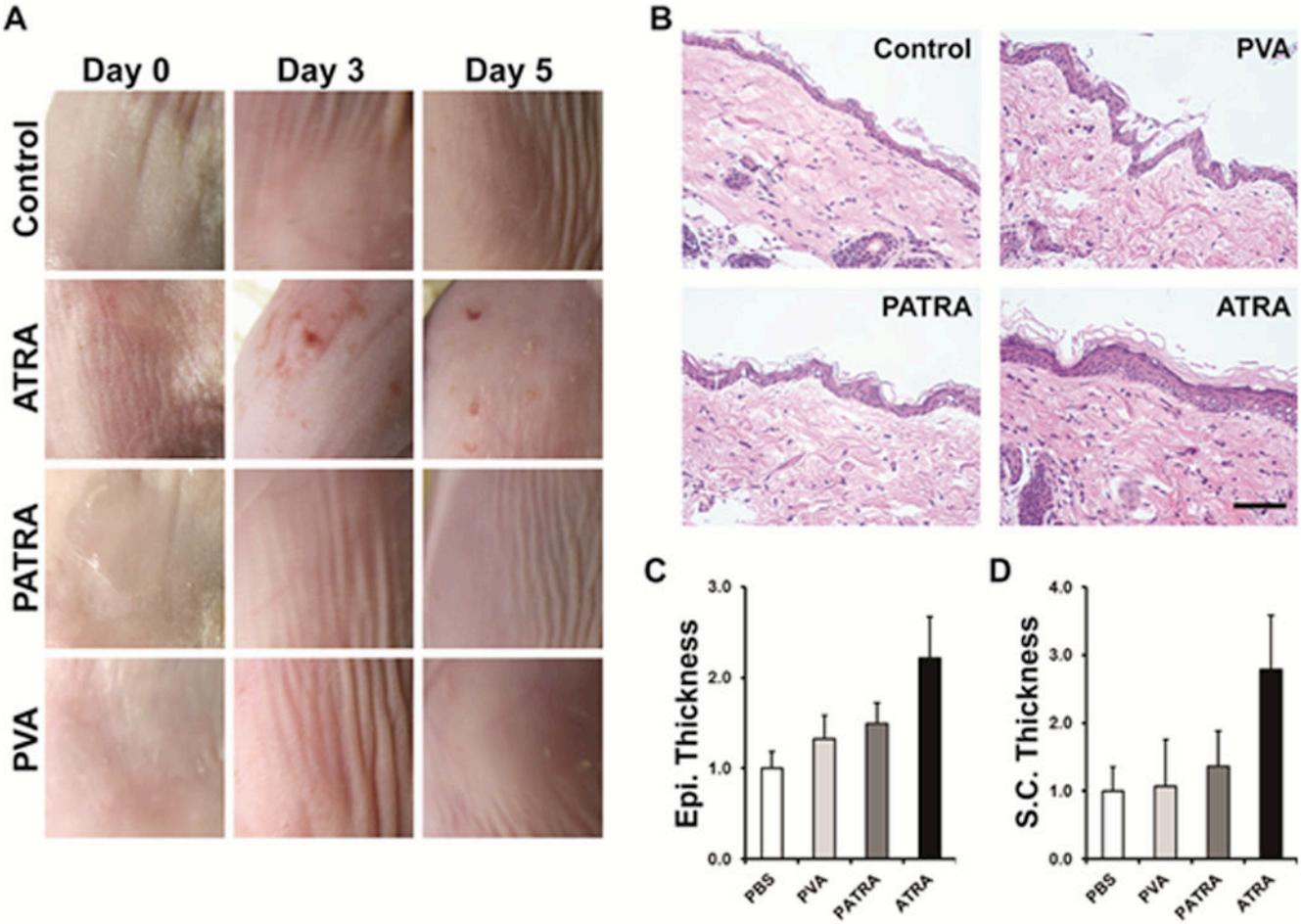

Figure 7. Reaction to ATRA application to the dermis

(a) Digital imaging of mouse dermis 0, 3, and 5 days post-application. (b) Histological sections of treated mouse dermis. Changes in epidermal and stratum corneum thickness are clearly observed due to bolus administration of ATRA. These changes are not observed in other treatment groups. (c-d) Quantification of histological findings for the treatment groups after five days. Data shown are mean ± S.D., n = 4.

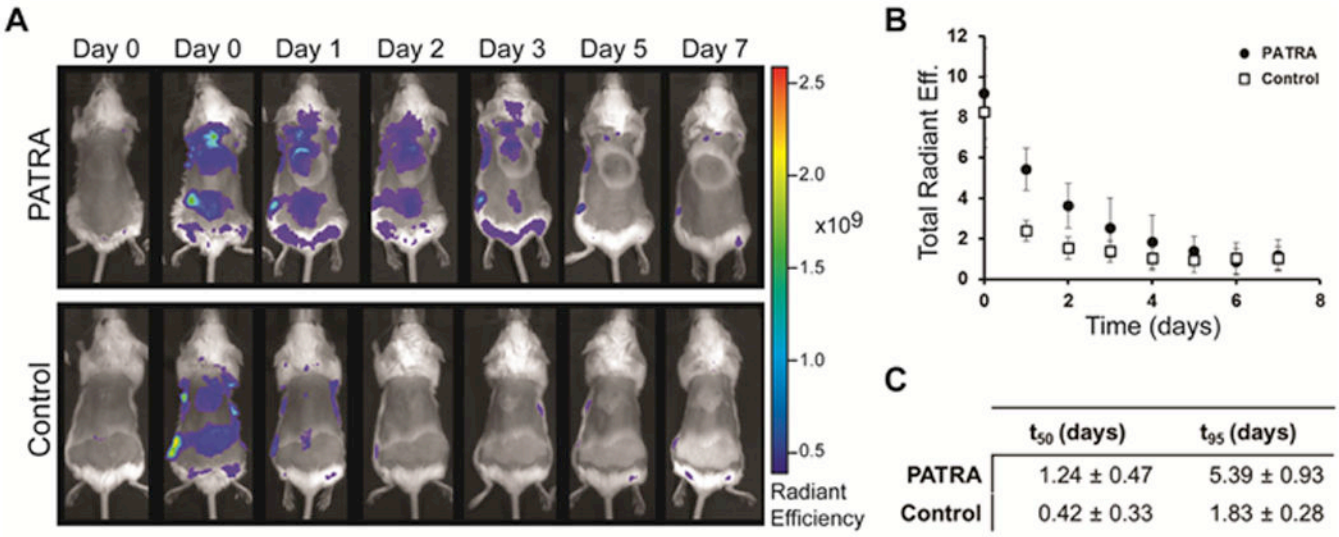

Figure 8. Retention of PATRA in the skin of mice

(a) IVIS imaging of fluorescently labeled PATRA over 7 days. Unconjugated dye is seen to disappear after only two days while PATRA conjugated dye stays for up to 5 days. Material was added at two locations on the midline of the backs of mice. (b) Quantification of total radiant efficiency for each application site for PATRA and dye treated mice. (c) Half-life and t_{95} measured from first-order exponential fits of fluorescent data. Data shown is mean ± S.D., n=6.